Astron. Astrophys. 326, 165–176 (1997)

ASTRONOMY
AND
ASTROPHYSICS

Stellar activity and the Wilson-Bappu relation

Øystein Elgarøy, Oddbjørn Engvold, and Per Jorås

Institute of Theoretical Astrophysics, Oslo, Norway

Received 1 April 1996 / Accepted 12 December 1996

Abstract. The Mg II h and k lines of 78 single stars observed with the International Ultraviolet Explorer (IUE) observatory have been analyzed. Stars of spectral classes F, G, K and M and luminosity classes I–V are represented in the sample. From these data it is shown that the Wilson-Bappu relation for the Mg II h and k lines is fulfilled over a range of 18 magnitudes, i.e. from M_v = +12 to M_v = -6.

The sample contains slowly rotating stars of different activity levels and is suitable for investigations of a possible relation between line width and stellar activity. It is found that active stars have broader lines and show a larger variation in line widths than quiet stars. Observations of the active RS CVn binary σGem taken at epochs when it shows different levels of activity, clearly demonstrate line broadening following higher activity.

Possible implications of the new results for the interpretation of the Wilson-Bappu relation are briefly discussed.

Key words: stars – chromospheres – coronae – activity

1. Introduction

The systematic broadening of the bright Ca II emission lines in spectra of late type stars (surface temperature equal to that of the Sun or cooler) with increasing stellar luminosity, which was first pointed out by Wilson and Bappu (1957), is of fundamental interest for the understanding of the temperature and density structure of outer stellar atmospheres.

McClintock et al. (1975) reported later on that a similar relation exists for the Mg II h and k lines and H Ly α, from observations of five K giants with the Copernicus satellite. Various W-B relations have been established by a number of authors (Kondo *et al.*, 1976; Stencel, 1977; Weiler and Oegerle, 1979; Engvold and Elgarøy, 1987; Vladilo et al., 1987).

From model calculations Ayres (1981) predicted that the FWHM of the Mg II h and k emission lines should be nearly independent of the activity of the star. In their study of high-resolution spectra of late-type stars from F5 to K5, and luminosity classes III - IV, Cerruti-Sola et al. (1992) concluded that there were no dependence of the Mg II k line widths on activity level. On the other hand, Montes et al. (1994) concluded from studies of Ca II H and K line widths in active binaries that the emission line widths for very active stars were larger than in less active stars. This also seems to agree with White and Livingston (1981) and Sivaraman et al. (1987) who found a small but significant increase in line width with solar activity. It is noted that in the cases of rapidly rotating stars the measured line widths are strongly influenced by rotational broadening. It is not clear how the inclusion of rapidly rotating stars in the study of Cerruti-Sola et al. may have overshadowed a possible activity dependent effect. In an attempt to resolve the seemingly contradicting results above, we have investigated the line width dependence on stellar activity based on a number of slowly rotating stars. Our sample covers a total range of 18 magnitudes, from +12 to -6, the spectral classes F, G, K and M and the luminosity classes I–V.

Since the initial detection by Wilson and Bappu, the physical basis for the width-luminosity relation has been vigorously debated. The two basic theories are based on assumptions about systematic effects in, (i) Doppler broadening with stellar absolute magnitude, or (ii) column density above the temperature minimum, respectively. Detailed discussions of the two suggestions are presented in papers by Ayres (1979), Linsky (1980) and Lutz and Pagel (1982). Engvold and Rygh (1978), and Engvold and Elgarøy (1987) presented evidence showing that the chromospheric mass column density, by its relation to the line opacity, is the dominant parameter for the Wilson-Bappu effect.

2. The data

The generation of the data base used in the present paper started out with an original sample of 17 cool giant and super-giant stars used in a study by Jorås (1989). Later, additional medium and low luminosity stars have been added, both from new IUE observations and by de-archiving the VILSPA data base, to make up the present set of nearly 80 stars.

The addition of the medium and low luminosity stars was done after a careful search in the Catalogue of Nearby Stars (Gliese, 1969). The following criteria were used in the selection process:

Send offprint requests to: Ø. Elgarøy

1. The stars should be evenly distributed over as wide a range as possible of spectral types and luminosity classes.
2. Both *active* and *quiet* stars should be represented.
3. Stars with Mg II lines severely affected by absorption in the local interstellar medium (LISM) should be avoided.
4. Stars with special peculiarities, such as high rotational velocities, severely affecting the line profiles, should be avoided.
5. Close binaries should be avoided, in particular all spectroscopic binaries.

The chromospheric emission weakens from cool to hotter stars and, as a consequence, only the photospheric absorption is visible in the spectrum. In K and M stars, the emission peaks are usually very strong and easily measurable. In early G stars, and particularly in F stars, the peaks weaken and become increasingly more difficult to measure. We therefore find no reason to investigate stars hotter than spectral type F.

The highest luminosity stars are usually easy to observe and have strong Mg II emission lines, but their profiles are always affected by central reversals due to self absorption in the outer extended stellar atmosphere or in circumstellar shells, or due to interstellar absorption. These "contaminations" often make determinations of the line profile parameters very difficult. The most luminous star in the sample is α Ori with $M_{\rm v} = -5.6$.

In the lower end of the luminosity scale the Mg II lines are often "clean" and show no self-reversals, but the stars are so weak that even with exposure times of several hours it is difficult to obtain a good signal to noise ratio. Because of the long exposure times needed relatively few high resolution spectral observations exist of these weak stars.

In our data sample there are a few stars that have been observed two or more times. In these cases we use mean values for the line profile parameters. In the case of two stars, σ Gem and α Ori, a large number of high resolution spectra are at at our disposal, since these stars have been studied in other programs dealing with long term spectral variability (Engvold et al., 1988; Jorås, 1989).

Items 2–4 above need a more detailed explanation, which is given below.

Stellar activity It is well known that stars of all luminosity classes show different levels of activity. *Active* stars are characterized by strong emission in the "hot" lines like C IV and Si IV, which originate in the transition region. These stars also have a hot corona and strong magnetic fields. *Quiet* stars, on the other hand, show little or no emission in these "hot" lines, only in "cool" chromospheric lines like O I, S I, Si II and Mg II. These stars have no transition region and consequently no corona, only a stellar wind, and the magnetic fields are weak. A few stars, termed *hybrid* stars, show some characteristics of both classes, having weak, but detectable transition region lines and rapid stellar winds.

The chromosphere-corona transition region lines are located in the short wavelength range of the IUE spectra covered by the SWP camera (1200–2000 Å). The Mg II lines at 2800 Å, on the other hand, are in the long wavelength region, covered by the LWR or LWP cameras (2000–3200 Å). Thus, only stars for which both SWP and LWR/P spectra are available can be readily classified as either quiet or active according to the above criterion. Unfortunately, not all LWR/P spectra are accompanied by SWP spectra. Of course, a number of stars are well known from earlier studies to be either active or quiet, such as the cool supergiants, the RS CVn stars, and the active dwarfs of the flare star type, but in general we cannot say *a priori* whether or not a given star is active. In general the Mg II surface flux may serve as an activity indicator.

We define a separation between *active* and *quiet* stars at a surface flux in the Mg II k line of $\log F_{\rm surf,k} = 5.2$ (see discussion later in this paper). Most main sequence stars are active.

LISM absorption The structure and dynamics of the Local Interstellar Medium (LISM) has been studied in a number of papers (Crutcher, 1982; Molaro et al., 1984, 1986; Vladilo et al., 1985). The LISM velocity, $v_{\rm LISM}$, in the direction (l^{II}, b^{II}), may be calculated with considerable confidence using the Crutcher relation:

$$\frac{v_{\rm LISM}}{v_{\rm LISM,0}} = \sin b^{II} \sin b_0^{II} + \cos b^{II} \cos b_0^{II} \cos(l^{II} - l_0^{II}) \qquad (1)$$

representing the uniform motion of a cloud with velocity $v_{\rm LISM,0} = 28\,{\rm km\ s^{-1}}$ in the direction $(l_0^{II}, b_0^{II}) = (25°, +10°)$ (Crutcher 1982; Vladilo et al., 1985). In this way we may choose stars for which $v_{\rm LISM}$ combines favorably with the stellar radial velocity $v_{{\rm r},*}$ in order to avoid severe contamination of the Mg II h and k line profiles. Recent work has shown that the kinematics of the LISM is more complex than implied by Eq. (1). However, within the limits of the velocity resolution of high resolution IUE data, it is still correct to make use of this equation.

The conditions used to select stars free of LISM absorption in the steepest part of the wings, defined to be the region 0.3–0.7 *FWHM* from the line center, are the following. We select stars that satisfy either $|v_{\rm LISM} - v_{{\rm r},*}| \leq 0.3 \times FWHM_{\rm pred}$, having absorption in the central region, or $|v_{\rm LISM} - v_{{\rm r},*}| \geq 0.7 \times FWHM_{\rm pred}$, having absorption in the far wings or completely outside the line. Here $FWHM_{\rm pred}$ is the full width at half maximum for the k line predicted from the star's $M_{\rm v}$, using the relations of Vladilo et al. (1987). This criterion of selection is rather crude since the $M_{\rm v}$ values often are poorly known and the actually measured width often deviates significantly from the predicted one. It was therefore no surprise to find that a few of the spectra turned out to be quite useless. These are subsequently discarded.

Stellar rotation The rotational rates of stars are discussed, for instance, by Gray (1992; Chapter 17). The so-called *rotation dividing line* runs diagonally across the lower half of the HR diagram from about F5 V to G2 III (Fig. 1). Crossing this line from left to right there is a very rapid drop to small rotational velocities of the order of 5–10 km s^{-1}. No such sharp boundary is seen in the upper half of the HR diagram, but stars cooler than about G0 I-II generally have moderate velocities of $\leq$ 20 km

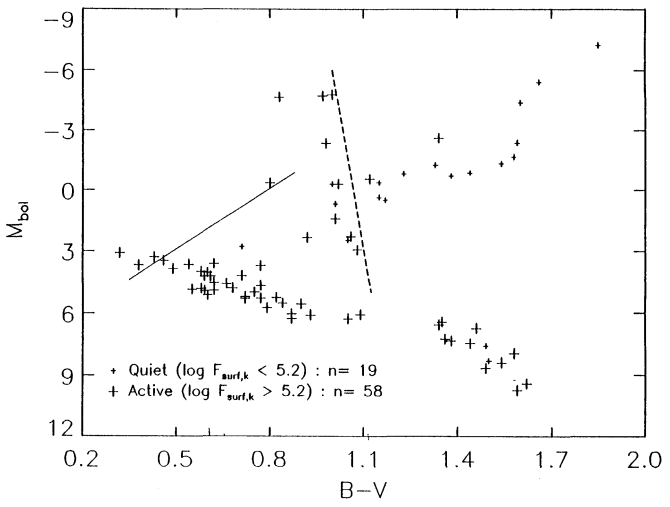

Fig. 1. The distribution of the stars in the HR diagram. A separation between *active* (large symbols) and *quiet* (small symbols) stars at log $F_{\rm surf,k} = 5.2$ is made. The *rotational braking line* and *coronal dividing line* are shown as solid and dashed lines, respectively.

$\rm s^{-1}$. Fig. 1 shows that practically all stars in our data set occupy this low or moderate velocity region. For the present study it is essential to use a sample of slowly rotating stars in order to eliminate broadening effects due to rotation (cf Montes et al. 1994).

We have examined the $v \sin i$ values listed in the Bright Star Catalogue (Hoffleit 1982) for all stars in our data set. Most G–K I-III stars are listed with $v \sin i \leq 17\,\rm km\ s^{-1}$. These stars have Mg II line widths of the order of 100–200 km $\rm s^{-1}$, and using a square correction for rotation ($W^2 = W^2_{\rm obs} - W^2_{\rm rot}$) we see that rotation has only a negligible effect on the Mg II widths for these stars. Thus the highest rotation rate (27 km $\rm s^{-1}$) in the RS CVn system σ Gem leads to only a 2 % correction in the Mg II width, which is well inside the expected error of measurement.

The remaining stars in our sample have either no listed value at all or rather small values for $v \sin i$, in accordance with their location in the slow-rotation region. Even the upper limits of $v \sin i \leq 17\,\rm km\ s^{-1}$ for a few stars would lead to corrections smaller than the expected errors of measurement in each case. Thus, when we restrict our data set to the slow-rotation region, all corrections for this effect are rather insignificant. These considerations justify our decision not to make any corrections at all for stellar rotation in our data.

Errors in stellar data Apart from the errors of measurement, there are also errors in some of the basic stellar data. The most important of these are the errors in the $M_{\rm v}$ values, which enter directly in the Wilson-Bappu type diagrams. We have compared the $M_{\rm v}$ values given in two catalogues: "Sky Catalogue 2000" (Hirshfeld and Sinnott, 1982) and "Catalogue of nearby stars" (Gliese, 1969; Gliese and Jahreiss, 1979), which are listed in Table 1. In most cases, the discrepancies are within a few tenths of a magnitude, but in 6 stars the differences are 2 magnitudes or more. The worst cases are GL 201 and GL 113.3, which appear in the listing with differences of 6 magnitudes. In these cases, the star is listed as a giant in one catalogue but as a dwarf in the other. The best way to treat such cases is to consider the widths of the Mg II lines and compare with other stars with similar profiles to select the best of the two $M_{\rm v}$ values. When the difference is as large as 6 magnitudes, it is usually a simple task to discard one value as erroneous. When the distinction is less clear we just adopt the Sky Catalogue 2000 values for the brightest stars and the Gliese values for the medium and weak stars. The discarded $M_{\rm v}$ values are put in parentheses in Table 1.

It is reasonable to assume that the adopted $M_{\rm v}$ values have uncertainties of the order 0–2 mag. Calculating the mean of the $M_{\rm v}$ differences for all stars that have two values listed (disregarding the two worst cases mentioned above) we arrive at $\delta M_{\rm v} \sim 1.0$ mag, which is regarded as a reasonable error estimate of the $M_{\rm v}$ values.

When the Hipparcos data are released in the near future, the precision in absolute magnitudes and distances will become much better, which hopefully will lead to improved definition of the relations derived in the present work.

A complete list of the stars is given in Table 1.

3. Data processing and analysis of the profiles

The data have been processed and analyzed using the British Starlink software (Bromage, 1984). The IUEDR program (Giddings, 1983; Giddings and Hook, 1985) is used to extract calibrated spectra from each IUE image. The standard calibrations of IUEDR are used in the process. Program DIPSO (Howarth, 1984) is used to analyze these extracted spectra. The main objective of the DIPSO analysis is to measure the widths and fluxes of the Mg II lines, using a least squares Gaussian fitting. Before line fitting, the photospheric flux level is subtracted and any defect parts of the spectrum, either due to bad pixels, "false lines" or absorptions, may be excluded from the fit (see Jorås 1989).

Since the data span a very large range of luminosities and temperatures, the appearance of the Mg II line profiles vary substantially. It is therefore difficult to find a single method to measure line profiles that is equally well suited to be used for all spectra. The conventional method, used by Vladilo et al. (1987), is to measure widths at an intensity of 50 % between the bottom (k_1 and h_1) and the top (k_2 and h_2) of the chromospheric emissions. The line fluxes may then be directly measured by an integration across the line profile. However, if the line is affected by LISM absorption, a certain fraction of the flux will be missing, and the usefulness of this method is considerably reduced. In such cases we have considered the alternative method of extrapolating the line profile with a Gaussian fit. A major problem is that it is often difficult to decide whether a reversal is due to LISM absorption only, or is formed in the stellar atmosphere itself. In many cases, it is a combination of the two. The methods considered are described below.

All line measurements start by subtracting the photospheric flux level and fitting that part of the line which is unaffected by a possible central reversal to a Gaussian (Fig. 2). This usually means a fit to the line wings (excluding the reversal). If there

Table 1. The observed stars

Star	Image[1]	[2]	Spec	M_v[3]	M_v[4]	B.C.	M_{bol}	B-V
β Dra	2 11087		G2II		-2.1	-0.24	-2.34	-0.98
	1 9933							
ζ Cap	2 13554		G4Ibpe		-4.5	-0.29	-4.79	1.00
56 Peg	2 14084		K0IIp		-2.1	-0.50	-2.60	1.34
α Aur	2 10257		G6III + F9III		0.0	-0.36	-0.36	0.80
λ And	2 14805		G8III-IV		1.8	-0.38	1.42	1.01
	2 16890							
β Cet	2 11372		K0III	(0.88)	0.2	-0.50	-0.30	1.02
	2 11373							
σ Gem	several	x	K1III		0.0	-0.55	-0.55	1.12
β Aqr	2 8935		G0Ib		-4.5	-0.16	-4.66	0.83
α Aqr	2 13538		G2Ib		-4.5	-0.22	-4.72	0.97
	2 13976							
α Tr A	1 6163		K3III		-0.1	-0.76	-0.86	1.44
λ Vel	2 14088		K5Ib		-4.4	-1.02	-5.42	1.66
	1 8331							
β Gru	2 14087		M3II		-2.4	-2.00	-4.40	1.60
α Ori	several	x	M1-2Ia-Iab		-5.6	-1.62	-7.22	1.85
α Boo	2 15752		K2III	(-0.25)	-0.2	-0.61	-0.81	1.23
	1 12787							
α Tau	1 12538		K5III	(-0.63)	-0.3	-1.02	-1.32	1.54
	1 12539							
β And	1 16750		M0IIIa	(0.33)	-0.4	-1.26	-1.66	1.58
	1 16877							
γ Cru	2 1356		M3III	(0.0)	-0.5	-1.87	-2.37	1.59
α Cen A	2 2097		G2V	(4.08)	4.4	-0.20	4.20	0.71
χ Ori	1 2235		G0V	(4.42)	4.4	-0.18	4.22	0.59
GL 783 A	1 21426	x	K3V	6.54	(6.6)	-0.50	6.04	0.87
GL 201	1 21251	x	K5Ve	6.80	(-0.1)	-0.72	6.08	1.09
GL 845	1 21252	x	K5Ve	7.01	(7.0)	-0.72	6.29	1.05
GL 142	1 21250	x	K7V	7.61		-1.01	6.60	1.34
GL 169	1 13950	x	M1Ve	8.08		-1.62	6.46	1.35
GL 825	1 13952	x	M0Ve	8.75		-1.38	7.37	1.38
GL 616.2	1 8262		M1.5Ve	8.38		-1.62	6.76	1.46
GL 803	2 13553		M0Ve	8.87		-1.38	7.49	1.44
GL 96	1 19848	x	M1.5Ve	9.11		-1.50	7.61	1.49
GL 239	1 19849	x	M1V	9.71	(9.6)	-1.38	8.33	1.50
GL 867 A 1	1 14210	x	M2Ve	10.3		-1.62	8.68	1.49
GL 867 A 2	1 14210	x		11.0				
GL 388	1 8278		M4.5Ve	10.98		-2.55	8.43	1.54
GL 799	several	x	M4.5Ve	10.53		-2.55	7.98	1.58
GL 867 B	1 14209	x	M4Ve	11.80		-2.38	9.42	1.62
GL 285	1 8281		M4.5Ve	12.29		-2.55	9.74	1.59
70 Vir	2 1945	x	G5IV-V	3.03	(5.2)	-0.24	2.70	0.71
θ Cen	2 4416		K0III-IV	1.12	(1.7)	-0.45	0.67	1.01
ϵ Ret	2 4417		K2IVa	3.49	(-0.3)	-0.55	2.94	1.08
η Cep	2 4427		K0IVe	2.74	(3.2)	-0.40	2.34	0.92
ν 2 CMa	2 4440-		K0IVe	2.70	(0.0)	-0.40	2.30	1.06

is no reversal, of course the whole line is fitted. We denote the spectral fluxes of the emission line and the Gaussian fit by F_λ and F'_λ, respectively. The corresponding peak fluxes are denoted I_0 and I'_0, which are the parameters that determine the flux level at which the line widths are measured. The line is usually partly asymmetric, and I_0 is measured at the highest of the two (red or violet) peaks. We let $\Delta(y)$ denote the full width of the line profile at the flux level y, and $\Delta'(y')$ the corresponding quantities for the Gaussian fit.

In the conventional method the width is defined as the full width of the line at the 50 % level of the peak line flux, $\Delta(I_0/2)$. However, since the spectrum usually is noisy and often difficult to define, even in the line wings, the actual measurement is better done at the Gaussian fit rather than at the emission line. Besides, the spectrum may in some cases be so asymmetric that

Table 1. (Continued)

Star	Image[5]	[6]	Spec	M_v[7]	M_v[8]	B.C.	M_{bol}	B-V
ϵ Sco	2 4444		K2III	0.97	(-0.1)	-0.61	0.36	1.15
72 Her	2 5317		G0V	4.70	(4.4)	-0.18	4.52	0.62
31 Aql	2 6308		G8IV	4.05	(3.2)	-0.34	3.71	0.77
α Ari	2 7067		K2IIIe	0.24	(-0.1)	-0.61	-0.37	1.15
	1 4039							
47 Uma	2 7350		G0V	4.39	(4.4)	-0.18	4.21	0.61
α Ser	2 7575		K2IIIe	1.10	(-0.1)	-0.61	0.49	1.17
61 Uma	2 10314		G8Ve	5.56	(5.5)	-0.26	5.30	0.72
ζ Tuc	2 10687		G0V	4.97	(5.0)	-0.18	4.79	0.58
	2 3699							
39 Tau	2 11724		G5V	5.09	(5.2)	-0.21	4.88	0.62
9 Cet	2 11851		G2V	4.78	(4.7)	-0.20	4.58	0.66
GL 117	2 11875		K0Ve	6.59	(6.6)	-0.31	6.28	0.87
	1 14453							
11LMi	2 13233		G8IV-Ve	5.58	(5.6)	-0.30	5.28	0.77
12 Oph	2 13311		K0V	5.55	(5.9)	-0.31	5.24	0.82
GL5	2 14654		K0Ve	5.29	(5.9)	-0.31	4.98	0.75
GL 761.1	2 16089		G5V	5.41	(5.2)	-0.21	5.20	0.72
GL 211	1 2107		K1Ve	5.89	(6.1)	-0.37	5.52	0.84
503.2	1 3101		G1.5Ve	5.31	(4.5)	-0.20	5.11	0.60
GL 224.1	1 4903		K3IV	2.97		-0.50	2.47	1.05
δ Sgr	1 5932		K2III	(0.98)	-0.1	-0.61	-0.71	1.38
κ Cet	1 6787		G5Ve	4.99	(5.0)	-0.21	4.78	0.68
GL 380	1 8279		K7Ve	8.29	(8.3)	-1.01	7.28	1.36
GL 113.1	1 11877		K0III	(5.15)	0.2	-0.50	-0.30	
α Ind	1 13105		K0III	(1.40)	0.2	-0.50	-0.30	1.00
44 And	2 16091		F8V	4.20	(4.0)	-0.16	4.04	0.60
6 Cet	1 2201		F6V	4.00	(3.7)	-0.15	3.85	0.49
ν Phe	1 2203		F8V	4.15	(4.0)	-0.16	3.99	0.58
β Cae	2 6299		F2V	3.80	(4.0)	-0.11	3.69	0.38
50 Per	2 14714		F7V	3.81	(3.8)	-0.15	3.66	0.54
ν 2 Col	1 2205		F2V	3.58	(3.0)	-0.11	3.47	0.46
GL 297.1	2 12858		F5V	3.44	(3.4)	-0.14	3.30	0.43
α Crv	2 10421		F2IV	3.22	(1.9)	-0.11	3.11	0.32
HN Peg	2 5013		G0Ve	5.08	(4.4)	-0.18	4.90	0.59
β Hyi	1 6404		G1IV	3.83	(3.8)	-0.21	3.62	0.62
	2 9686							
GL 259	1 24840	x	K0Ve	5.87	(5.9)	-0.31	5.56	0.90
GL309	1 24841	x	K0V	6.06	(6.1)	-0.31	5.75	0.79
GL 320	1 24842	x	K1V	6.48	(6.5)	-0.37	6.11	0.93
GL 454	1 24850	x	K0IV	5.07	(3.2)	-0.40	4.67	-0.77
GL484	1 24851	x	G0V	5.03	(4.4)	-0.18	4.85	0.55
GL593.1	1 24853	x	K4III	(3.37)	-0.3	-0.94	-1.24	1.33

Notes:
1) 1=LWP, 2=LWR
2) x = observed by the authors
3) Gliese(1969), Gliese & Jahreiss (1979)
4) Hirshfeld and Sinnott (1982): Sky Catalogue 2000

the lowest peak doesn't even reach the 50 % level. The quantity $\Delta(I_0/2)$ would then be meaningless, since it would give the width of the dominating peak rather than the width of the whole line. By using the Gaussian fit as an extrapolation to "fill in" the missing flux we obtain a much better estimate of the width. The flux is then defined as the integrated flux under the line profile. Thus, we define

$$W = \Delta'(I_0/2) \tag{2}$$

$$F = \int F_\lambda d\lambda. \tag{3}$$

In the alternative method the width is defined as the full width of the fit at 50 % of its peak level, and the flux is defined

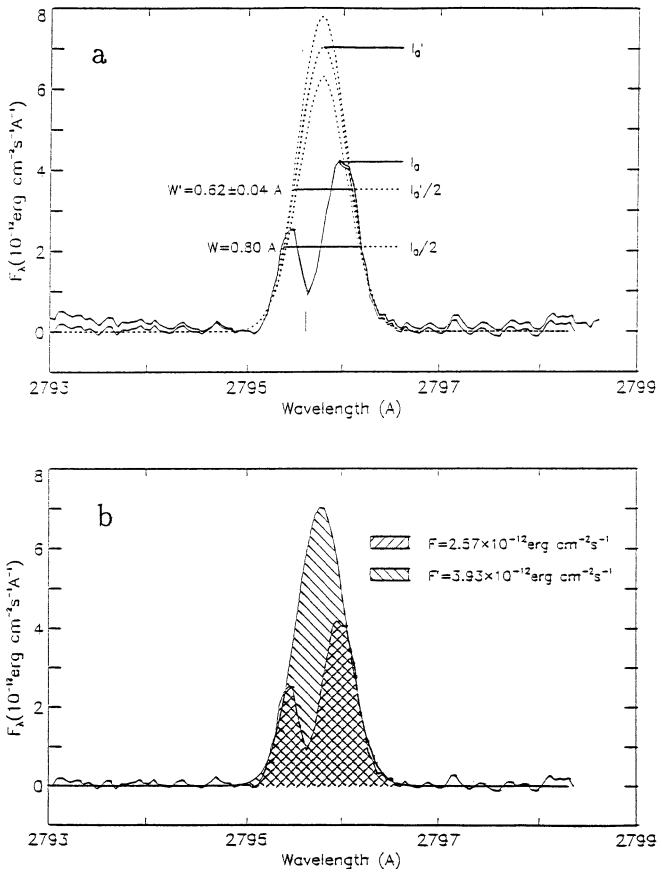

Fig. 2a and b. The measurement of line profiles, using ϵ Ret as an example. **a** illustrates the two methods for line width measurement. The emission line profile is shown both before and after correction for the photospheric flux level. The predicted relative position of the LISM absorption, indicated by the vertical bar, coincides closely with the observed reversal. Three possible Gaussian fits to the corrected lines, with reversal excluded, are made by slightly changing the positions of the cutoff points limiting the central reversal region, thus giving an empirical error estimate of W'. **b** illustrates the two methods for measuring fluxes. (The wavelength scale is relative to the IUE frame of reference, since no correction for the spacecraft velocity has been made.)

as the integrated flux under the Gaussian fit

$$W' = \Delta'(I'_0/2) \tag{4}$$

$$F' = \int F'_\lambda d\lambda. \tag{5}$$

Normally, three independent fits are made by slightly changing the positions of the cutoff points that limit the excluded central reversal. The largest and smallest of these fits are taken to represent the range of possible fits, and thus give an estimate of the errors in the line fitting process. Finally, the line widths and fluxes W' and F' are calculated as weighted means of the three fits.

In a method which has been extensively used the width at the base of the emission, $W'' = \Delta(0)$ is measured. The advantage of this method is that it is unaffected by self reversals, but because the k_1 and h_1 minima usually are not well defined in the IUE spectra we find it useless. In some cases, however, it may be used as a test method for comparison with other methods.

The conventional method (Eqs. 2 and 3) has the advantage that there are no extrapolations and that the actual measurements can be carried out with rather high precision. If the central reversal is due to absorption in the stellar atmosphere itself, then some or all of the flux that is missing from the line center may be redistributed to the wings. Then the directly integrated F is a much better flux estimate than the extrapolated F'. On the other hand, if the central reversal is due to absorption in the local interstellar medium, the absorbed flux is totally removed from the line, and the extrapolated flux F' is the best estimate.

All lines in our sample have been measured using the two methods illustrated in Fig. 2. The parameter F is used a the primary flux estimate. Both W and W' are used as alternative width parameters, and the results are compared. All derived line widths are corrected for the instrumental broadening, using a square correction ($W^2 = W^2_{obs} - W^2_{inst}$), where W_{inst} = 21 km s^{-1} at the wavelength of the Mg II lines (Turnrose and Thompson, 1984). It should be noticed that the width of the narrowest lines in the spectra are near to the width of the instrument profile. Hence, a small error in the measurement of the observed FWHM causes a larger error in the determined intrinsic width of the chromospheric line. An error estimate for these lines has previously been made by Elgarøy (1988) and Elgarøy et al. (1990). Furthermore, if the instrumental FWHM has been over-estimated, the line width of the faintest dwarfs would be under-estimated. We rely on the value given by Turnrose and Thompson for the instrumental profile, but even if its width was over-estimated by an amount corresponding to several km s^{-1} it would not invalidate our conclusions.

In addition to the errors introduced by detector noise and uncertainties in the interpretation of the central reversal of the line profiles, some spectra are also affected by pixel saturation and reseau marks in the Mg II lines. In particular, the Mg II k line at 2795Å is affected by a reseau mark in a number of LWP spectra. In these cases, the errors of measurement are correspondingly increased.

4. Results

4.1. The Wilson-Bappu relation for Mg II

Fig. 3 shows the width-luminosity relation of the Mg II h and k lines for our sample of 78 stars observed with IUE. In each case, two least squares regression lines are calculated, one for M_v versus $\log W$ and one for $\log W$ versus M_v, and the mean of the two lines is adopted as the final regression line shown as a solid line on each plot. The correlation coefficient r is independent of the order of the two parameters and is written on each plot together with an equation for the mean regression line of the form $M_v = A \log W + B$.

The error estimates $\delta W'$ are shown as horizontal error bars on Fig. 3c,d together with a single vertical error bar giving the magnitude error δM_v. No error bars are plotted on Figs. 3a and

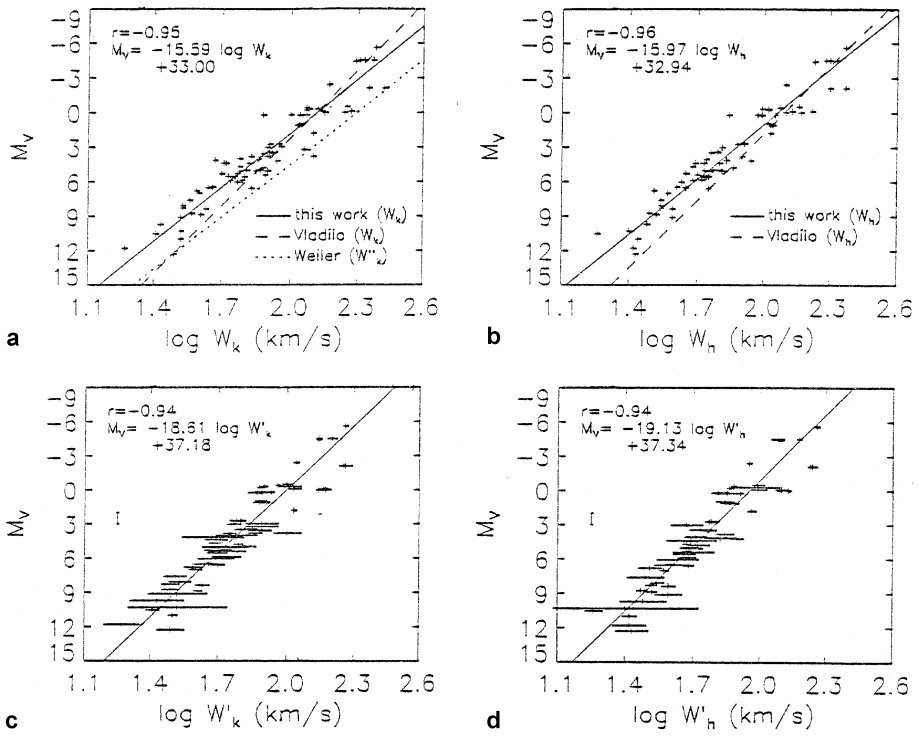

Fig. 3a–d. The width-luminosity relation of the Mg II h and k lines, using both W (**a,b** top) and W' (**c,d** bottom) as width parameters. The regression lines are plotted as solid lines, and their equations are written on the plots, together with the correlation coefficients. For comparison, the regression lines of Vladilo *et al.* and Weiler & Oegerle are also shown. The horizontal error bars show the estimated width errors in each point, while the single vertical error bar is a rough estimate of the general error in the absolute magnitude.

b. The errors in W are expected to be smaller than the errors in W'.

The Figures clearly show that the absolute magnitude and width follow a relation of the type $M_{\rm v} = A \log W + B$. The correlation coefficient is close to -0.95 in all cases. A conclusion derived from our sample of 78 stars is that the Wilson-Bappu relation for Mg II is valid over the entire range of 18 magnitudes, i.e. from M_v = +12 to M_v = -6.

We have also plotted the regression lines found by Vladilo et al.(1987) (dashed line) and Weiler & Oegerle (1979) (k line only, dotted) in Fig. 3a,b.

When comparing the results it is important to notice that different line width parameters are used. For the strongly reversed profiles of the brightest stars, $W > W'$, while for the weakest stars there is no such difference. This leads to a smaller slope $|A|$ in Figs. 3a and b than in c and d. The Weiler & Oegerle (WO) line is based on $\log W''_{\rm k}$ rather than $\log W_{\rm k}$, giving systematically larger widths, but the slope is basically the same as our slope for $W_{\rm k}$. In this sense the two datasets are consistent.

Vladilo et al. used the same definition as applied in the present work ($W_{\rm k}$, $W_{\rm h}$), so the results should be directly comparable. But the slope of the Vladilo data is steeper than found by us. However, it is very close to the slopes we find when using W'_k and W'_h. W' may be a better choice than W since W' is best for luminous stars and W and W' give identical results at low luminosities. Another possible reason for these small discrepancies in slope is the fact that the sample of Vladilo et al. covered a smaller range in M_v (M_v from -1 to +7) than the sample used in the present investigation.

At this point it is interesting to note that the slopes found by other workers for Mg II and Ca II lines are all in the range -14.7 to -15.2, although the methods of measurement differ (Wilson and Bappu, 1957; Mc Clintock et al., 1975; Engvold and Rygh, 1978). When the width parameter W' is used the resulting slope for Mg II is slightly steeper than for Ca II. This might imply that the Ca II H and K, and the Mg II h and k lines are formed in slightly different chromospheric layers. For lines formed at quite different heights, different slopes of M_v to $log\ W_o$ would be expected, as was actually found by Stencel (1977). A discussion of the physical reasons behind the slopes of the various W-B relations is of substantial interest, but should be based on large samples of high precision data. Hipparcos data will be invaluable for this task.

Interesting differences are revealed in the spread in the data of Vladilo et al. (1987), Weiler and Oergerle (1979) and the present data. Since they do not cover the same $M_{\rm v}$ ranges, a direct comparison requires that we consider only the range $-1 < M_{\rm v} < 6$, which is common to all data. The correlation coefficients for the WO, Vladilo and our data restricted to this range are -0.72, -0.95 and -0.86, respectively. Another useful parameter is the total width deviation from the mean relation, which is roughly 0.30, 0.10 and 0.30 for the three datasets. Thus, the WO data show somewhat lower correlation than our data, which was expected because of the poor quality of the Copernicus data compared to IUE spectra. On the other hand, the Vladilo data show remarkably good correlation, and much smaller spread than our data. The reason for this difference is not clear, but it could be a result of the way the stars were selected. A possible explanation could be that our data generally contain

more active stars than the Vladilo data, since active stars show larger variations in widths, as discussed in Sect. 4.3.

In conclusion, our data satisfy a Wilson Bappu type relation of the form $M_v = A \log W + B$, valid for M_v = +12 to −6. The slope A is in the same general range as that found by other workers, even though A is ≈-19 for Mg II when W' is used.

4.2. Stellar activity parameters

4.2.1. The Mg II surface flux: a direct activity measure

One of the most direct activity parameters would be the strength of the transition region (TR) lines relative to the chromospheric (CHR) lines. However, to measure these lines we need SWP high resolution spectra, which are unavailable for all but about 20 of the stars, mostly giants and supergiants. We may then consider the Mg II k line surface flux (the flux measured at the stellar surface) since this is accessible from all spectra, although it is not expected to be as strong an indicator of stellar activity as the TR to CHR flux ratio. The surface flux is obtained from the observed flux (in cgs units) using the formula

$$F_{\rm surf} = (4/\Theta^2) F_{\rm obs} = 1.70 \times 10^{17} F_{\rm obs}/\theta^2 \quad (6)$$

where Θ and θ are the stellar angular diameters measured in radians and milli-arcseconds, respectively. Observed values of θ are used, if available, otherwise they are calculated from the stellar distance and radius. Distances are adopted from the Sky Catalogue 2000 (Hirshfeld and Sinnott, 1982) or the Catalogue of Nearby Stars (Gliese, 1969). Stellar radii are derived from

$$\log(R/R_\odot) = -0.2 M_{\rm bol} - 2 \log T_{\rm eff} - 8.451 \quad (7)$$

(Lang, 1992, 9.2) where $M_{\rm bol} = M_v$ + BC, while BC and $T_{\rm eff}$ are adopted from Lang (1992, 9.7). We estimate the error in the derived surface fluxes to amount to approximately 50%, corresponding to an uncertainty of 0.3 in the logarithm of the surface flux.

The TR flux, $F_{\rm tr}$, is defined as the sum of the fluxes of N V 1238–43, Si IV 1393–1402 and C IV 1548–50; the CHR flux, $F_{\rm chr}$, as the sum of O I 1302–06, S I 1807–26 and Si II 1808-17. All these lines are found in the SWP spectra. To test the usefulness of the Mg II k line surface flux as an activity parameter, $\log F_{\rm surf,k}$ versus $F_{\rm tr}/F_{\rm chr}$ for those 23 stars for which we have high resolution SWP spectra, is plotted in Fig. 4a. Supergiants, giants and dwarfs are distinguished by the size of the symbols. The RS CVn system σ Gem has been observed a number of times, and the measured range of variation of both parameters are indicated by the inclined solid bar. The horizontal dotted bar indicates the uncertainty of the flux ratio for α Cen A caused by strong saturation of the SWP spectrum above 1800 Å.

The *quiet* stars, characterized by complete absence of TR lines ($F_{\rm tr}/F_{\rm chr} = 0$), all cluster in the lower left of the diagram, below about $\log F_{\rm surf,k} = 5.0$, while the *active* stars, with substantial TR fluxes, are in the upper part, above $\log F_{\rm surf,k} = 5.2$. The only exceptions to this pattern are the three *hybrid* stars, marked by asterisks (∗). They all have very small, but detectable TR fluxes, although one of them, the giant α Tr A, has weak

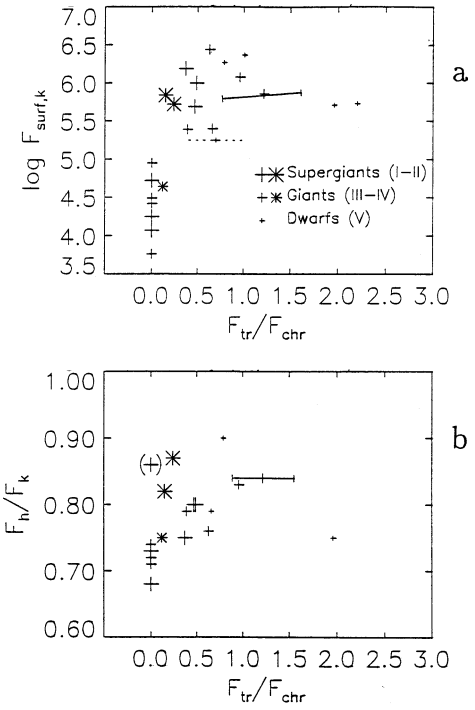

Fig. 4. a the Mg II k line surface flux versus flux ratio of hot (transition zone) to cold (chromospheric) lines for the 23 stars for which high resolution SWP spectra are available. The symbol size indicates luminosity class. The inclined solid bar shows the range of variations of σ Gem, while the horizontal dotted bar indicates that the flux ratio for α Cen A is very uncertain because of strong saturation of the SWP image above 1800 Å. The three *hybrid* stars are marked by asterisks. There is a clear separation between *quiet* stars ($F_{\rm tr}/F_{\rm chr} = 0$) in the lower part, and *active* stars ($F_{\rm tr}/F_{\rm chr} > 0$) in the upper part of the Figure. We define the separation between these two classes to be at $\log F_{\rm surf,k} = 5.2$. **b** the same as in **a** but the flux ratio $F_{\rm h}/F_{\rm k}$ is plotted along the ordinate instead of $\log F_{\rm surf,k}$.

Mg II surface flux like the quiet stars, while the supergiants α Aqr and β Aqr have strong surface fluxes like the active stars.

These 23 stars represent all spectral and luminosity classes of this study, even though the dwarfs are somewhat underrepresented. Therefore, we find it reasonable to assume that the pattern shown here is of a more general validity. We may then introduce a separation between active and quiet stars at a constant value of $\log F_{\rm surf,k}$ of, say, 5.2. Thus, stars above this line are defined as active, those below as quiet. The obvious advantage of such a definition is that the Mg II fluxes are available for all stars in our sample, in contrast to the TR fluxes.

Certainly, such a sharp division is artificial, since there actually seems to be a continuous transition from quiet to active stars. Nevertheless, this two-level model is very useful for easy visualization of important differences between the two groups. The exact position of the separation is somewhat arbitrary, depending on which property we choose to characterize stellar activity. Therefore, one may adjust the value $\log F_{surf,k} = 5.2$ somewhat up or down to better illustrate special effects.

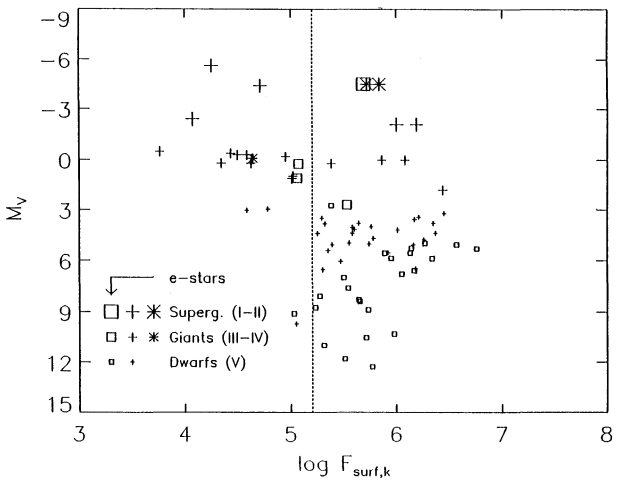

Fig. 5. The distribution of the stars according to absolute magnitude and Mg II k-line surface flux. As in Fig. 4, symbol sizes indicate luminosity classes. Stars with e-suffix in the spectral type (emission line stars) are marked by squares. The vertical dotted line at log $F_{\rm surf,k}$ = 5.2 defines our separation between *quiet* (to the left) and *active* stars (to the right).

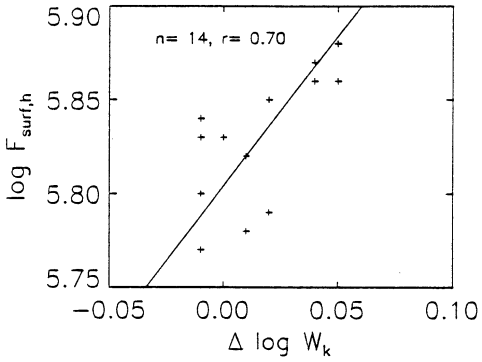

Fig. 6. The Mg II activity (log $F_{surf,h}$ versus width deviations ($\Delta log\ W_k$) of the Mg II k-line, defined as the difference between the measured width and the least squares fit to the data shown in Fig. 3a.

Our adopted value of 5.2 may, perhaps, seem somewhat low compared to the results of Cerruti-Sola et al. (1992) for the Sun and stars. They found no difference between Mg II surface fluxes of quiet solar regions and coronal holes. The "average" fluxes for quiet and active (plage) regions were found to be log $F_{\rm surf,k}$ = 5.8 and 6.7, respectively. In a flare the flux might be even larger. There was a considerable spread in the solar values.

The data of Cerruti-Sola et al. (1992) comprise 55 stars of spectral class F5 to K5 and luminosity class IV or V, with log $F_{\rm surf,k}$ ranging from 5.5 to 7.0. These are thus all *active* stars according to our definition. In comparison, the stars of luminosity class V in our dataset range from about 5.0 to 6.8 (Fig. 5). We also note that the more luminous stars in Fig. 5 show a much larger range of activity than the dwarfs. In particular, a number of the giants and supergiants have *very* low surface fluxes.

4.2.2. The Mg II h/k ratio: as a measure of activity

In addition to the Mg II surface flux, the Mg II h/k line flux ratio may be readily determined from the IUE spectra. It is therefore of interest to see if the ratio can be used as a measure of activity.

The ratio of the Ca II H and K line fluxes is indicative of chromospheric optical depth and temperature gradients (Kelch et al., 1978, 1979). The Mg II h to k line flux ratio $F_{\rm h}/F_{\rm k}$ can also be used as a measure of opacity. This ratio is expected to lie between 0.5 and 1.0, corresponding to the optically thin and thick cases, respectively. It is generally believed that opacity plays a major role in the general widening of the lines with increasing luminosity (Elgarøy et al., 1990).

Moreover, as will be demonstrated below, there is a close connection between the widening of lines and stellar activity. This means that we would expect $F_{\rm h}/F_{\rm k}$ to be a relevant parameter for measuring stellar activity.

In Fig. 4b this ratio is plotted versus $F_{\rm tr}/F_{\rm chr}$ for the same sample of stars as in Fig. 4a (the number of points is somewhat smaller since the flux ratio could not be measured in all cases). A general increase in the h/k flux ratio with increasing activity as measured by $F_{\rm tr}/F_{\rm chr}$ is clearly seen. Also, there seems to be a separation at about $F_{\rm h}/F_{\rm k}$ = 0.75, in the sense that stars above this line have $F_{\rm tr}/F_{\rm chr} > 0$ and are thus active, while stars below this line are quiet.

In our data we find a relatively weak variation of the line flux ratio F_h/F_k with surface flux (activity level). This could mean that the latter is the result of an increase in the fractional area covered by active regions, as also suggested by Cerruti-Sola et al. (1992), rather than local changes in thickness of an active chromosphere. Thus, $F_{surf,k}$ seems to be a more direct and reliable activity parameter than the flux ratio F_h/F_k.

4.3. The Wilson-Bappu relations for quiet and active stars

The very active RS CVn star σGem has been observed by these authors several times in connection with another project (Engvold et al. 1988; Elgarøy et al. 1995). Since the activity of this star varies, it is well suited for a study of the relation between activity and Mg II h and k line widths. In Fig. 6 the results of 14 observations are shown. The usual parameter $log\ F_{surf,k}$ is replaced by $log\ F_{surf,h}$ since the k-line in several cases was over-exposed. The least squares regression line reveals larger line width with higher activity. This is an important result since errors in surface fluxes are minimized because all measurements refer to the same star.

It is now a matter of interest to see if the effect of activity is revealed in the Wilson-Bappu relation of the Mg II lines. For this purpose the material was divided in two groups, quiet and active stars, respectively, according to surface flux in the Mg II k-line. The respective width-luminosity relations are shown in Fig. 7a,b. (In the Figure the parameter $W^{'}$ is used since it may be best for luminous stars (cf. Sect. 3). But W may, of course, also be used. However, W and $W^{'}$ are in practice equivalent at low luminosities.) Both quiet and active stars are seen to

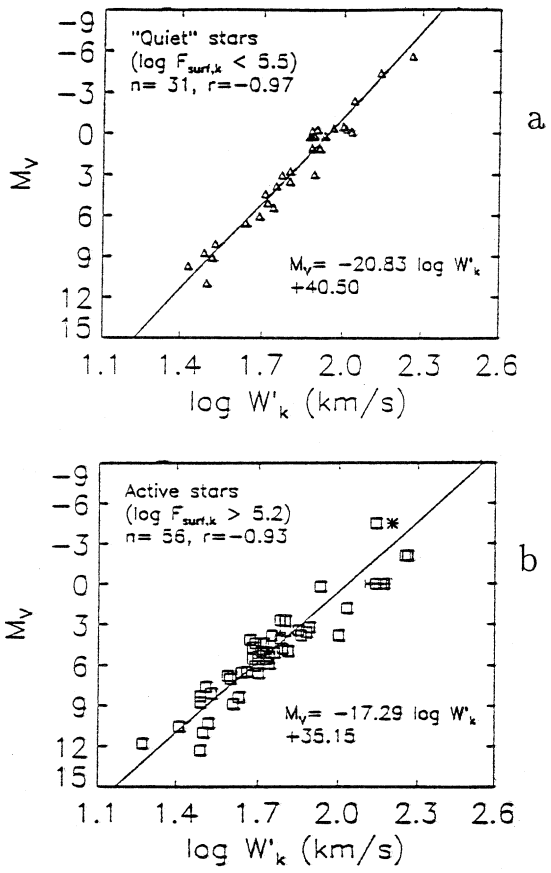

Fig. 7a and b. The width-luminosity relation for quiet and active stars, using W_k' as the width parameter. **a** shows the plot for the quiet stars, while the active stars are shown in **b**. The asterisk ($*$) marks the position of the two hybrids α and β Aqr, which are coincident. Not that in order to obtain a larger number of stars in a we have pushed the limit between quiet and active stars up to $logF_{surf,k}$ = 5.5. In both diagrams the correlation coefficient is high. Accordingly, the uncertainties in the coefficients for the linear regression line become rather small. In the case of panel b they amount to $\pm$0.88 and $\pm$1.54, for the slope and constant, respectively. For the upper panel the uncertainties are nearly the same, being $\pm$0.80 and $\pm$1.44.

follow Wilson-Bappu relationships. The Figure reveals some interesting differences between the two groups.

The active stars apparently show a somewhat larger spread in line widths than the quiet stars (Fig. 7a and b). An alternative and maybe better illustration of this increased variation in widths is given in the plot of log $F_{\rm surf,k}$ versus Δ log $W_{\rm k}$ in Fig. 8. Note that $\Delta logW_k$ is defined as the difference between the measured width and the least squares fit to the data shown in Fig. 3a. This should not be confused with the definition of deviation used in Elgarøy et al. (1990) which was relative to the fit of Vladilo et al. (1987).

The slope of the regression line for the active stars is smaller than for the quiet stars. Active giants and supergiants appear to have significantly wider Mg II lines than those that are quiet.

The most important information contained in Fig. 7 is thus that active high luminosity stars have substantially broader lines

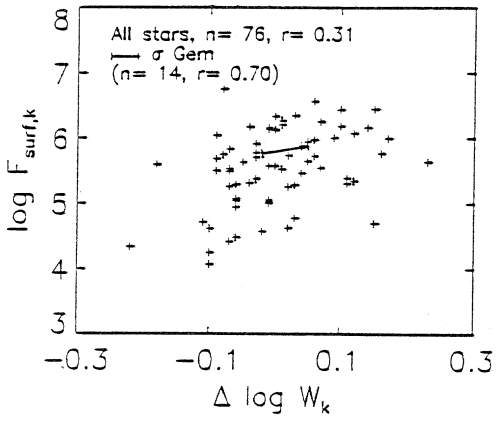

Fig. 8. The Mg II activity (log $F_{\rm surf,k}$) versus the width deviation (Δ log W_k) of the Mg II k line, defined as the difference between the measured width and the least squares fit to the data shown in Fig. 3a. The range of variations of $\sigma\ Gem$ is indicated by the inclined bar.

than quiet stars, and show greater variation in line widths. This variation is mostly due to the large range of activity levels from star to star. However, since stellar activity is closely connected with variability, such as in UV Ceti stars (flare stars) and the active binaries of the RS CVn and BY Dra types, some of the variation is very likely a result of the changing levels of activity on each individual star. Long-term observations of a selected sample of stars would be of interest (cf σGem).

This Section has demonstrated that stellar activity is affecting the line widths. This is clearly borne out from our observations of σGem and confirmed by the comparison between quiet and active stars in our sample. Thus, the Wilson-Bappu relation should be modified to include an activity term, in analogy with the relation of Lutz and Pagel (1982), who expressed the line width in terms of fundamental atmospheric parameters such as gravity, effective temperature and metallicity.

5. Discussion and concluding remarks

We have analyzed the spectra and measured Mg II h & k line profile parameters of 78 stars observed with the IUE satellite. With a very few exceptions these are all single stars with low to moderate rotational velocities. They are also all selected so as to avoid serious absorption by interstellar Mg II in the line wings. The strong central reversals in luminous stars make the determination of line profile parameters difficult. Therefore, two alternative methods of measuring widths and fluxes are considered. The present data represent an improvement in amount and quality, and span a larger range of absolute magnitudes as compared with earlier work.

The measured broadening of the chromospheric emission lines with absolute stellar magnitude follows the Wilson-Bappu relation over almost 18 magnitudes. The Mg II h and k lines follow a Wilson-Bappu type relation of the form $M_{\rm v}$ = A log W + B, valid for the whole range from $M_{\rm v}$ = +12 to $M_{\rm v}$ = $-$6. The slope A is about -16 when the line widths are determined in the conventional way. But when W' is used, which seems to be the

best width parameter for the entire range in luminosities, the slope becomes steeper with $A \approx$-19.

From high resolution spectrographic observations of the RS CVn binary system HR 1099 (primary star K1 IV) Wood et al. (1996) find enhanced emission in the wings of Mg II h & k. They suggest that micro flaring activity and associated turbulence may affect the wings of both chromospheric and transition region lines. The micro flaring activity must be quite substantial in order to affect the FWHM of the line profiles. The line widths are in the range $1.25 \leq \log W_k \leq 2.30$, which in the case of turbulence corresponds to velocities ranging from about 20 km s^{-1} to 200 km s^{-1}. In the event that the chromospheric turbulence increases from the lower to the upper chromosphere (Harper 1992) an increasing line broadening from turbulence may follow an increasing opacity. The widths of optically thin chromospheric lines correspond to about 10 km s^{-1} (Engvold and Elgarøy 1987), which then may represent the non-thermal velocities in the lower chromospheres.

The assumption that non-thermal motions control the Mg II line profiles would imply a highly supersonic turbulence. The sound speed in the stellar chromospheres is expected to be less than 15 km s^{-1} (at temperature T $\approx 10^4$ K). (In the transition region the sound speed is about 30 km s^{-1}.) Recent numerical modeling of the Ca II H_2 and K_2 grains in the solar chromosphere shows that these line profiles could result from outward propagating acoustic waves that form shocks and dissipate their energy (Carlsson and Stein 1995). It is not yet clear what the situation will be in magnetic flux tubes, but future modeling including magnetic fields may show whether or not the Wilson-Bappu relation may reflect flux tube dynamics (cf. Rutten 1995). However, radiative transfer modeling suggests that the Wilson-Bappu effect can be explained by chromospheric opacity (Qing Qi-cheng 1996).

It has been shown that the Mg II h and k surface fluxes characterize quite well the stellar activity level. The stars may be classified as active stars when the parameter $\log F_{surf,k} \geq 5.2$ [cgs units]. Non-active stars fall below this set limit. The line flux ratio F_h/F_k, on the other hand, which should be an indicator of optical thickness, show very weak correlation with activity. The reason for this is presumably that for optical thickness $\tau_{MgII\ k} \leq 10^6$ (see Elgarøy et al. 1990) the line is effectively optically thin. For opacities less than this value the emergent line flux is not noticeably dependent on τ (Elgarøy et al. 1990).

The Mg II k line surface flux may be used as an activity parameter, instead of the strength of the transition region lines, which in many cases are unavailable because of lack of SWP spectra. This is in agreement with the results of Cerruti-Sola *et al.* (1992). There is a continuous transition from the most quiet ($\log F_{\rm surf,k} \sim 3.7$) to the most active ($\log F_{\rm surf,k} \sim 6.8$) stars. Although there is no sharp limit between quiet and active stars, we have chosen $\log F_{\rm surf,k} = 5.2$ as the "best value".

Dwarfs are generally more or less active, since they almost all have $\log F_{\rm surf,k} > 5$, whereas amongst giants and supergiants there are both quiet and active stars.

Active stars generally have wider lines than less active stars. Moreover, the intrinsic variation in line widths seems to be larger for active stars. This is a combined effect of the large ranges of activity between different stars, and the variability of individual stars. An example of this is the RS CVn variable σ Gem, which has wider lines at high activity than at low.

References

Ayres, T.R. 1979, ApJ, 228, 509
Ayres, T.R. 1981, ApJ, 244, 1064
Bromage, G.E., 1984, 4th European IUE Conference, ESA SP-218, 473
Carlsson, M, and Stein, R. 1995, in Proceedings of "The 9th Cambridge Workshop on Cool Stars, Stellar Systems and the Sun", Florence, 3-6 October 1995. Eds.: R.Pallavicini and A. Dupree (in press)
Cerruti-Sola, M., Cheng, C.-C., Pallavicini, R. 1992, A&A, 256, 185
Crutcher, R.M. 1982, ApJ, 254, 82
Elgarøy, Ø. 1988, A&A, 204, 147
Elgarøy, Ø., Jorås, P., Engvold, O., Jensen, E., Pettersen, B.R., Ayres, T.R., Ambruster, C., Linsky, J.L., Clark, M., Kunkel, W., Marang, F. 1988, A&A, 193, 211
Elgarøy, Ø., Engvold, O., Carlsson, M., 1990, A&A, 234, 308
Elgarøy, Ø., Engvold, O., Jorås, P. 1991, "Proceedings from the NSSR Annual Meeting" Møn, Denmark, Ed.: P. Høeg, ISBN 87-7478-308-4, p 183
Elgarøy, Ø., Engvold, O., Jorås, P. 1995, Poster Proceedings from IAU Symp. 176, Vienna, Ed.: K.G.Strassmeier, p 165
Engvold, O., Rygh, B.O. 1978, A&A, 70, 399
Engvold, O., Elgarøy, Ø. 1987, Fifth Cambridge Workshop on Cool Stars, Stellar Systems and the Sun, Lecture Notes Phys., 291, 315
Engvold, O., Ayres, T.R., Elgarøy, Ø., Jensen, E., Jorås, P.B., Kjeldseth-Moe, O., Linsky, J.L., Schnopper, H.W., Westergård, N.J. 1988, A&A, 192, 234
Giddings, J. 1983, ESA IUE Newsletter, 17, 53
Giddings, J., Hook, R.N. 1985, Starlink User Note 37, Rutherford Appleton Laboratories, London
Gliese, W. 1969, Catalogue of nearby stars. Veröffentlichungen des Astronomiscen Rechen-Instituts Heidelberg Nr.22. Karlsruhe: Verlag G. Braun
Gliese, W., Jahreiss, H. 1979, A&AS, 38, 423
Gray, D.F. 1992, The observation and analysis of stellar photospheres, 2nd ed. Cambridge: Cambridge University Press
Harper, G.M. 1992, Mon. Not. Roy. Astr. Soc., 256, 37
Hirshfeld, A., Sinnott, R.W. 1982, Sky Catalogue 2000.0. Sky Publishing Corporation
Hoffleit, D. 1982, Bright Star Catalogue. Yale University Observatory
Howarth, I.D. 1984, Starlink User Note 50, Rutherford Appleton Laboratories, London
Jorås, P.B. 1989, Dr. Scient Thesis, Univ. Oslo
Kelch, W.L., Linsky, J.L., Basri, G.S., Chiu, H.Y., Chang, S.H., Maran, S.P., Furenlid, I. 1978, ApJ, 220, 962
Kelch, W.L., Linsky, J.L., Worden, S.P., 1979, ApJ, 229, 700
Kondo, Y., Morgan, T.H., Modisette, J.L. 1976, ApJ, 207, 167
Lang, K.R. 1992, Astrophysical Data: Planets and Stars. Springer-Verlag
Linsky, J.L., Haisch, B.M. 1979, ApJ, 229, L27
Linsky, J.L. 1980, Ann. Rev. Astron. Astrophys., 18, 439
Lutz, T.E., Pagel, B.E.J. 1982, MNRAS, 199, 1101
McClintock, W., Henry, R.C., Moos, H.W. 1975, ApJ, 202, 733
Molaro, P., Beckman, J.E., Crivellari, L., Franco, M.L., Vladilo, G. 1984, 4th European IUE Conference, ESA SP-218, 139
Molaro, P., Vladilo, G., Beckman, J.E. 1986, A&A, 161, 339

Montes, D., Fernandez-Figueroa, M.J., De Castro, E., and Cornide, M. 1994, A&A, 285, 609
Qing Qi-cheng 1996, In preparation
Rutten, R.J. 1994, Abstract of IAU Symposium 176, "Stellar Surface Structure". Vienna 9 - 13 Oct. 1995 (p. 54)
Sivaraman, K.R., Singh, J., Bagare, S.P., and Gupta, S.S. 1987, Ap. J., 313, 456
Stencel, R.E. 1977, ApJ, 215, 176
Turnrose, B.E., and Thompson, R.W. 1984, IUE Processing Information Manual Version 2.0, CSC/TM-84/6058
Vladilo, G., Beckman, J.E., Crivellari, L., Franco, M.L., Molaro, P. 1985, A&A, 144, 81
Vladilo, G., Molaro, P., Crivellari, L., Foing, B.H., Beckman, J.E., Genova, R. 1987, A&A, 185, 233
Weiler, E.J., Oegerle, W.R. 1979, ApJS, 39, 537
White O.R. and Livingston, W.C. 1981, Ap. J., 249, 798
Wilson, O.C., Bappu, M.K.V. 1957, ApJ, 125, 661
Wood, B.E., Harper, G.H., Linsky, J.L., and Dempsey, R.C. 1996, ApJ, 458, 761

This article was processed by the author using Springer-Verlag LaTeX A&A style file *L-AA* version 3.